Two-Metal Ion Mechanism of Bovine Lens Leucine Aminopeptidase: Active Site Solvent Structure and Binding Mode of L-Leucinal, a *gem*-Diolate Transition State Analogue, by X-ray Crystallography[†,‡]

Norbert Sträter and William N. Lipscomb*

Gibbs Chemical Laboratory, Harvard University, Cambridge, Massachusetts 02138

Received July 27, 1995; Revised Manuscript Received September 19, 1995[⊗]

ABSTRACT: The three-dimensional structures of bovine lens leucine aminopeptidase (blLAP) complexed with L-leucinal and of the unliganded enzyme have been determined at crystallographic resolutions of 1.9 and 1.6 Å, respectively. Leucinal binds as a hydrated *gem*-diol to the active site of blLAP, resembling the presumed *gem*-diolate intermediate in the catalytic pathway. One hydroxyl group bridges the two active site metal ions, and the other OH group is coordinated to Zn1. The high-resolution structure of the unliganded enzyme reveals one metal-bound water ligand, which is bridging both zinc ions. Together, these structures support a mechanism in which the bridging water ligand is the attacking hydroxide ion nucleophile. The *gem*-diolate intermediate is probably stabilized by four coordinating bonds to the di-zinc center and by interaction with Lys-262 and Arg-336. In this mechanism, Lys-262 polarizes the peptide carbonyl group, which is also coordinated to Zn1. The Arg-336 side chain interacts with the substrate and the *gem*-diolate intermediate via water molecules. Near Arg-336 in the blLAP−leucinal structure, an unusually short hydrogen bond is found between two active site water molecules.

Bovine lens leucine aminopeptidase (blLAP)[1] is a hexameric enzyme of molecular mass 324 kDa (Melbye & Carpenter, 1971; Carpenter & Harrington, 1972). The three-dimensional structures of the native enzyme (Burley et al., 1990, 1992) and of its complex with the inhibitors bestatin (Burley et al., 1991, 1992), amastatin (Kim & Lipscomb, 1993a), and L-leucinephosphonic acid (LeuP; Sträter & Lipscomb, 1995) have been determined previously (Figure 1). On the basis of these structures, three alternative mechanisms have been discussed, which share as common features a metal-bound hydroxide ion nucleophile and polarization of the carbonyl group by the zinc ions (Figure 2; Sträter & Lipscomb, 1995). In an attempt to differentiate between these possible pathways, we now report on two new X-ray structures of blLAP. First, the structure of unliganded blLAP is reported here from a crystallographic data set collected at cryogenic temperatures at 1.6 Å resolution, in order to determine the active site water structure including the possible positions of the water nucleophile. Second, we present the structure of blLAP complexed with the aminoaldehyde hydrate of L-leucinal, which resembles the presumed *gem*-diolate transition state of LAP catalysis more closely than does any of the previously determined transition state analogues (Figure 1). Both structures contribute new aspects to the discussion of the catalytic mechanism of LAP.

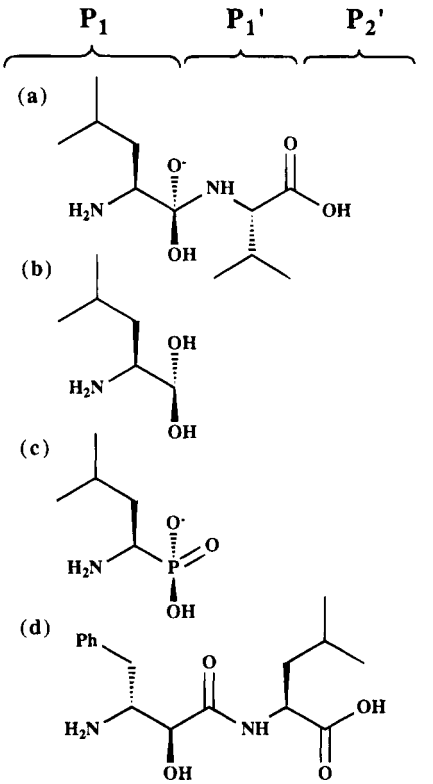

FIGURE 1: Transition state and inhibitors of LAP catalysis: (a) *gem*-diolate transition state of substrate L-leucyl-L-valine; (b) L-leucinal; (c) L-leucinephosphonic acid; and (d) bestatin.

Leucine aminopeptidase [LAP: α-aminoacyl-peptide hydrolase (cytosol), EC 3.4.11.1] is an exopeptidase that catalyzes the removal of amino acids from the N terminus of a peptide [for reviews, see Smith and Hill (1960), Delange and Smith (1971), Hanson and Frohne (1976), and Kim and

[†] This work was supported by NIH Grant GM 06920 (W.N.L.). N.S. thanks the Deutsche Forschungsgemeinschaft for financial support.

[‡] The coordinates have been deposited in the Brookhaven Protein Data Bank, Brookhaven National Laboratories, Upton, Long Island, NY, under file names 1LAM and 1LAN.

* Author to whom correspondence should be addressed.

[⊗] Abstract published in *Advance ACS Abstracts,* November 1, 1995.

[1] Abbreviations: LAP, leucine aminopeptidase; blLAP, bovine lens leucine aminopeptidase; LeuP, L-leucinephosphonic acid; MPD, 2-methyl-2,4-pentanediol; rms, root mean square; *B* factor, temperature factor; F_o and F_c, observed and calculated structure factors; O_n and O_c, oxygen atoms of the transition state from the former water nucleophile and former peptide carbonyl O, respectively; Zn1, site 1 zinc ion (Zn-488 in the coordinate file); Zn2, site 2 zinc ion (Zn-489).

0006-2960/95/0434-14792$09.00/0

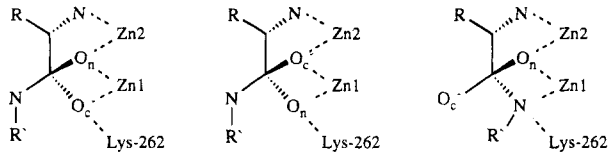

FIGURE 2: Three plausible mechanisms for LAP catalysis (left, mechanism I; middle, mechanism II; right, mechanism III). Only the binding mode of the transition state to the di-zinc center is schematically shown. O_c originally was the carbonyl oxygen, whereas O_n was the nucleophile arising from a water molecule. A more detailed formulation of these pathways is given in Sträter and Lipscomb (1995).

Lipscomb (1994)]. Aminopeptidases are ubiquitous in nature and are of critical biological and medical importance because of their key role in protein modification and degradation, and in metabolism of biologically active peptides (Taylor, 1993a,b). Altered aminopeptidase activity has been associated with several pathological disorders such as cancer (Umezawa, 1980) and possibly eye lens cataracts (Taylor et al., 1982).

Each of the six identical 54 kDa subunits of blLAP contains two zinc ions (Carpenter & Vahl, 1973) that are essential for catalytic activity and that display different exchange kinetics. The two metal ions are 2.9 Å apart in the native enzyme (Burley et al., 1990). The readily exchangeable site 1 can stoichiometrically bind Zn^{2+}, Mn^{2+}, Mg^{2+}, or Co^{2+} (Carpenter & Vahl, 1973; Thompson & Carpenter, 1976a,b; Allen et al., 1983) and has been identified as Zn1 in the structure determination of the Zn^{2+}–Mg^{2+} metallohybrid enzyme (Kim & Lipscomb, 1993). The zinc ion in the tight binding site 2 can be exchanged against Co^{2+} only when both binding sites are unoccupied (Thompson & Carpenter, 1976b; Allen et al., 1983). In contrast to some earlier results, it is now apparent that metal substitution in both binding sites significantly affects both K_m and k_{cat} (Allen et al., 1983). Thus, both metals participate in substrate binding and activation, including a possible role in the activation of the nucleophile.

A number of different reaction coordinate analogue inhibitors have been reported to bind to LAP. The structures of blLAP complexed with bestatin, amastatin, and LeuP showed that these inhibitors bind similar to the di-zinc center of the enzyme. The terminal amino group of the substrate coordinates to Zn2, the tight binding site 2 metal ion, and one of the P1 oxygen atoms bridges both metal ions. A new aspect of the structure of the blLAP–LeuP complex was the additional interaction of a second phosphoryl oxygen atom with Zn1. On the basis of this structure, it was proposed that both oxygen atoms of the *gem*-diolate intermediate coordinate to the dimetal center (mechanisms I and II, Figure 2). Alternatively, the coordination site at Zn1 might be occupied by the former peptide amino group in the transition state (mechanism III). Mechanisms I and II differ in the position of the attacking water nucleophile: in mechanism I, the nucleophile is a hydroxide ion bridging both zinc ions. In the transition state, this oxygen atom (O_n) also bridges both metal ions. The former carbonyl oxygen (O_c) is coordinated to Zn1. In mechanism II, the water nucleophile is a hydroxide ion coordinated to Zn1 and stabilized by a hydrogen bond from Lys-262. In this transition state model, O_c, the former carbonyl oxygen, bridges both metal ions.

Aminoaldehydes are strong inhibitors of LAP. L-Leucinal inhibits cytosolic aminopeptidase from porcine kidney with an inhibition constant of K_i = 60 nM (Andersson et al., 1982). Deuterium substitution in the aldehyde group of the inhibitor showed no effect on the inhibition constant, indicating that the amino aldehyde binds as an oxygen adduct, not as the intact aldehyde (Andersson et al., 1985). Since there are no nucleophilic amino acid side chains in the active site of blLAP that could attack the substrate carbonyl group in a double displacement mechanism, it appears most likely that the aminoaldehydes bind as a hydrated *gem*-diol, resembling an intermediate after direct attack of a water molecule on the scissile peptide bond of the bound substrate.

Besides blLAP, two other aminopeptidases employing a two-metal ion center in catalysis have been structurally characterized: *Aeromonas proteolytica* aminopeptidase (AAP) with a dinuclear zinc site (Chevrier et al., 1994) and the cobalt enzyme methionine aminopeptidase (Roderick & Matthews, 1993). The active site structures of all three structurally characterized aminopeptidases each containing a dimetal center are significantly different and obviously constitute different types of proteolytic enzymes.

The use of cryogenic temperatures in data collection facilitates the determination of water positions due to the reduced mobility (dynamic disorder) of the water molecules and due to the enhanced crystallographic resolution as a result of the minimized crystal decay in the X-ray beam. Exogenous water ligands coordinated to the di-zinc core could not be established in the previous structure of native blLAP at 2.3 Å resolution with data collected at ambient temperature. The structure of the unliganded enzyme presented herein allows for the localization of a zinc-bound water ligand, which is also proposed to be the attacking hydroxide ion nucleophile in LAP catalysis. The structure of blLAP complexed with L-leucinal corroborates the conclusions drawn from the binding mode of LeuP to blLAP and—in conjunction with the structures of the previous blLAP–inhibitor complexes and the now determined active site water structure—favors the proposed mechanism I (Figure 2).

MATERIALS AND METHODS

Enzyme Preparations. blLAP was isolated from bovine calf eye lenses according to the method of Carpenter (Allen et al., 1983). The enzyme was crystallized by equilibrating a hanging drop (20 μL) of 7 mg/mL blLAP, 50 μM $ZnSO_4$, 200 mM NaCl, and 50 mM Tris·HCl, pH 7.8, against a solution of 1:1 (v/v) 50 mM Tris·HCl/50 μM $ZnSO_4$–2-methyl-2,4-pentandiol (MPD) (Jurnak et al., 1977). Within 2 weeks, hexagonal, rodlike crystals of dimensions 1.0 × 0.35 × 0.35 mm appeared. One crystal was directly mounted from the drop for data collection. For the data collection of the blLAP–leucinal complex, a native blLAP crystal was incubated for 15 min with a solution of 20 mM L-leucinal in the crystallization buffer.

Inhibition by Sodium Bicarbonate. Specific activity was measured using L-leucine *p*-nitroanilide as substrate. Assay solutions consisted of 67 μg/mL enzyme, 0.5–5 mM substrate, 0.0–100 mM $NaHCO_3$, 200 mM NaCl, 50 mM Tris·HCl, pH 7.8, and 50 μM $ZnSO_4$. Solutions for activity tests in the absence of $NaHCO_3$ were degassed under vacuum. Release of *p*-nitroaniline was detected by the absorbance at 405 nm. Kinetic parameters were determined by double-reciprocal plots.

Synthesis of L-*Leucinal.* To a solution of 19 mmol of CBZ-L-leucine (Sigma) in 100 mL of anhydrous acetone were added 28.5 mmol of potassium carbonate and then 28.5 mmol of dimethyl sulfate, and the mixture was stirred under nitrogen at room temperature. The reaction was complete after about 2 h. The reaction mixture was diluted into 500 mL of ethyl acetate and washed with saturated $NaHCO_3$. The organic phase was dried over Na_2SO_4 and taken to dryness; yield, 17 mmol (90%) of CBZ-L-leucine methyl ester. The ester was reduced to CBZ-L-leucinal with diisobutylaluminum hydride by the procedure of Ito et al. (1975). CBZ-L-leucinal was purified by flash chromatography on silica gel eluted with $CHCl_3$ ($R_f = 0.35$). The CBZ group was removed by hydrogenolysis using the procedure given by Moriya et al. (1982). After the catalyst was removed by filtration, the resulting reaction mixture of L-leucinal in methanol was concentrated under vacuum at 25 °C to $\sim^1/_5$th of the reaction volume. Water was added (2 × reaction volume), and the solution was again concentrated. This procedure was repeated 2 times and yielded a solution of L-leucinal hydrochloride in water. Due to the reactivity of the aminoaldehyde, the solution was not evaporated to dryness. At pH 3 or below, this solution is stable for a few days at 4 °C: NMR (in D_2O, 500 MHz Bruker NMR spectrometer) δ 0.85 [6 H, q, J(vicinal) = 6 Hz, CH-(CH_3)$_2$], 1.4 (3 H, m, $CH_2CH<$), 3.2 (1 H, m, $>CHNH_2$), 5.0 [1 H, d, $J = 4$ Hz, $CH(OH)_2$], and 9.5 (1 H, s, CHO). A concentrated aqueous solution of L-leucinal was diluted to 20 mM at 0 °C in the crystallization buffer. The mixture was quickly titrated to pH 7.8, and the crystals were immediately soaked in the solution. Relatively short incubation times were used because at neutral pH concentrated solutions of the aminoaldehyde form yellow to red–brown-colored products within minutes.

Data Collection and Processing. X-ray diffraction data were collected at −150 °C on a Siemens X-1000 multiwire area detector. Monochromated Cu K_α radiation was produced by an Elliot GX3 rotating anode generator with a 200 μm focus cup operating at 35 kV and 40 mA and a Supper double-mirror system of two nickel-coated glass mirrors. A Siemens LT-2 low-temperature apparatus was used to maintain the temperature. The crystal was mounted in a hair loop free standing film of the MPD crystallization solution. Details of data collection and data reduction are summarized in Table 1. The program XDS was used for data reduction (Kabsch, 1988).

The coordinates of the native structure of blLAP were used as the starting model. Crystallographic refinement was performed using X-PLOR (Brünger, 1992a). Ten percent of the measured reflections were set aside throughout all refinement steps and used to calculate the free R-factor (Brünger, 1992b). The position of the protein in the unit cell was improved by rigid body refinement. Subsequent refinement was performed using alternating rounds of manual rebuilding and positional minimization. All model building was done with the program O (Jones & Kjeldgaard, 1994). Solvent molecules were included gradually from $F_o - F_c$ electron density maps if the peak height was stronger than $4\sigma_{rms}$ and the position was near (2.5–3.5 Å) a suitable hydrogen bonding donor or acceptor. Inclusion of additional water molecules from $F_o - F_c$ maps was stopped when the R_{free} did not decrease in the subsequent minimization run. The model for L-leucinal was included in the refinement after most of the protein was already well-refined and the difference electron density ($F_o - F_c$) for the inhibitor was well-defined. The refinement parameters for leucinal and MPD were determined using QUANTA (Molecular Simulations Inc., 1994). In this refinement, the zinc–ligand distances were not restrained, and the van der Waals radii of the zinc ions were set to zero. This procedure guarantees that the refined metal–ligand distances are not subject to any bias. The matrices for a superposition of different blLAP models or subunits were calculated by a least-squares distance minimization algorithm implemented inside the program O using the C_α-atoms as the guide coordinates, even if the rms difference has been analyzed for other atom types. Details of the refinement are listed in Table 1. Figures 5 and 7–8 were prepared using MOLSCRIPT (Kraulis, 1991), and Figures 3 and 6 were calculated using O (Jones & Kjeldgaard, 1994).

Table 1: Details of Data Collection and Refinement

	unliganded blLAP	blLAP–leucinal
Data Set Statistics		
space group	$P6_322$	$P6_322$
cell axes (Å)	$a = 131.5$, $c = 121.3$	$a = 131.2$, $c = 120.9$
max resolution (Å)	1.6	1.9
no. of crystals	1	1
temp (°C)	−150	−150
reflections measured	357105	160257
unique reflections	76376	44837
completeness (%)[a]	94.4 (83.2)	99.3 (99.2)
completeness > $2\sigma_F$ (%)[a]	84.8 (60.1)	87.5 (71.1)
R_{sym}[a]	0.070 (0.30)	0.070 (0.20)
V_m (Å^3/Da)	2.8	2.8
Refinement Statistics		
resolution range (Å)[a]	7.0–1.6 (1.65–1.6)	7.0–1.9 (2.0–1.9)
R/R_{free}	0.172/0.204	0.168/0.212
protein atoms (Z > 1)	3702	3702
water molecules	510	384
ligand atoms	28	33
rmsd		
bond length (Å)	0.011	0.010
bond angles (deg)	1.8	1.7
dihedral angles (deg)	21.9	22.1
improper twist angles (deg)	1.35	1.41
average B		
protein (Å^2)	12.2	16.3
waters (Å^2)	24.0	28.7
ligand (Å^2)	10.1	23.9
MPD (Å^2)	18.2	26.2
Ramachandran plot outliers	0	0

[a] The values in parentheses are for the highest resolution shell.

RESULTS

blLAP–Leucinal. The final refined structure of the blLAP–leucinal complex contains 484 amino acid residues, 3 zinc ions, 1 leucinal molecule, 3 MPD molecules (2-methyl-2,4-pentanediol), and 384 water molecules in the asymmetric unit. Three side chains (Arg-156, Cys-344, and Met-454) were found and refined in alternate conformations. The model shows good stereochemistry (Table 1), and the Luzzati plot (Luzzati, 1952) indicates a coordinate error of 0.15–0.2 Å. As in the previously reported structures of blLAP, there was no interpretable electron density for the C-terminal residues 485–487.

Leucinal Binding Mode. One molecule of leucinal binds to the active site of blLAP (Figures 3–5, Table 2). The 1.9

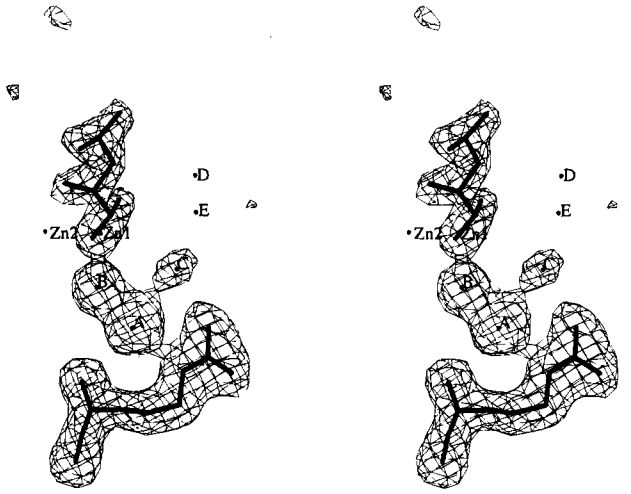

FIGURE 3: $F_o - F_c$ electron density map of Arg-336 (bottom), the active site water molecules A–C, and leucinal (top). These residues have been omitted from the refined model in the calculation of the density. Also shown are the two zinc ions and waters D and E. The contour level of the map is $2.5\sigma_{rms}$. At a higher contour level, the water molecules A and B show separated density.

Å electron density map shows clearly that leucinal binds in the hydrated form and not as the intact aldehyde. The terminal amino nitrogen is coordinated to Zn2. One of the *gem*-diolate oxygens, O1, bridges both metal ions, and the other oxygen, O2, is coordinated to Zn1. A water molecule (B) is hydrogen bonded to O1, the backbone nitrogen of Gly-335, the backbone carbonyl oxygen of Leu-360, and to water molecule A. In addition, water molecule A displays two hydrogen bonds to Arg-336 and to a third active site water, C. Also, water C has additional hydrogen bonding interactions with Arg-336 and with the carbonyl group of Leu-360.

Water molecule B displays a relatively short hydrogen bond to water molecule A as well as to O1 of leucinal (Figure 4). In order to obtain coordinates for the positions of water molecules A and B that are unbiased by the force field restraints usually employed in crystallographic refinement of proteins, we also refined these two water molecules without force field interactions with each other and with all other atoms, such that their positions are solely influenced by the X-ray data. Under these conditions, an even smaller distance between water molecules A and B of 2.3 Å is obtained. The distance between water molecule B and O1 of leucinal remains 2.5 Å. Waters A and B have *B*-factors of 3.2 and 13.2 Å^2, respectively, indicating that both positions are unlikely to be only alternatively occupied.

The two active site metal ions in the blLAP–leucinal complex are coordinated by six ligands in a distorted octahedral coordination geometry (Figures 4 and 5). However, as in the previous structures, $O_\delta1$ of Asp-255 is only weakly coordinated to Zn2. The two zinc ions have similar temperature factors of 11.7 Å^2 in site 1 and 14.2 Å^2 in site 2. The metal–metal distance is 3.2 Å. This distance is 3.1, 3.3, and 3.4 Å in the blLAP complexes with bestatin, amastatin, and LeuP, respectively.

Structure of the Unliganded Enzyme. The final refined structure of the blLAP–leucinal complex contains 484 amino acid residues, 3 zinc ions, 3 MPD molecules, and 510 water molecules in the asymmetric unit. Two side chains (Asp-291 and Cys-344) were found and refined in alternate conformations. The model shows good stereochemistry (Table 1), and the Luzzati plot indicates a coordinate error of 0.15 Å. No interpretable electron density was visible for the C-terminal residues 485–487. This structure is in good agreement with the previously refined structure of native blLAP crystallized from lithium sulfate solution (Burley et al., 1990, 1992), and both structures superimpose with an rms deviation of 0.37 Å for the C_α-coordinates (Figures 4, 6, and 7). The zinc–zinc distance was refined to 3.0 Å. Zn1 and Zn2 have temperature factors of 9.7 and 9.3 Å^2, respectively. Both blLAP structures reported herein show the presence of a third metal ion (binding site 3), which has been refined as a zinc ion to *B*-factors of 21.8 and 35.2 Å^2

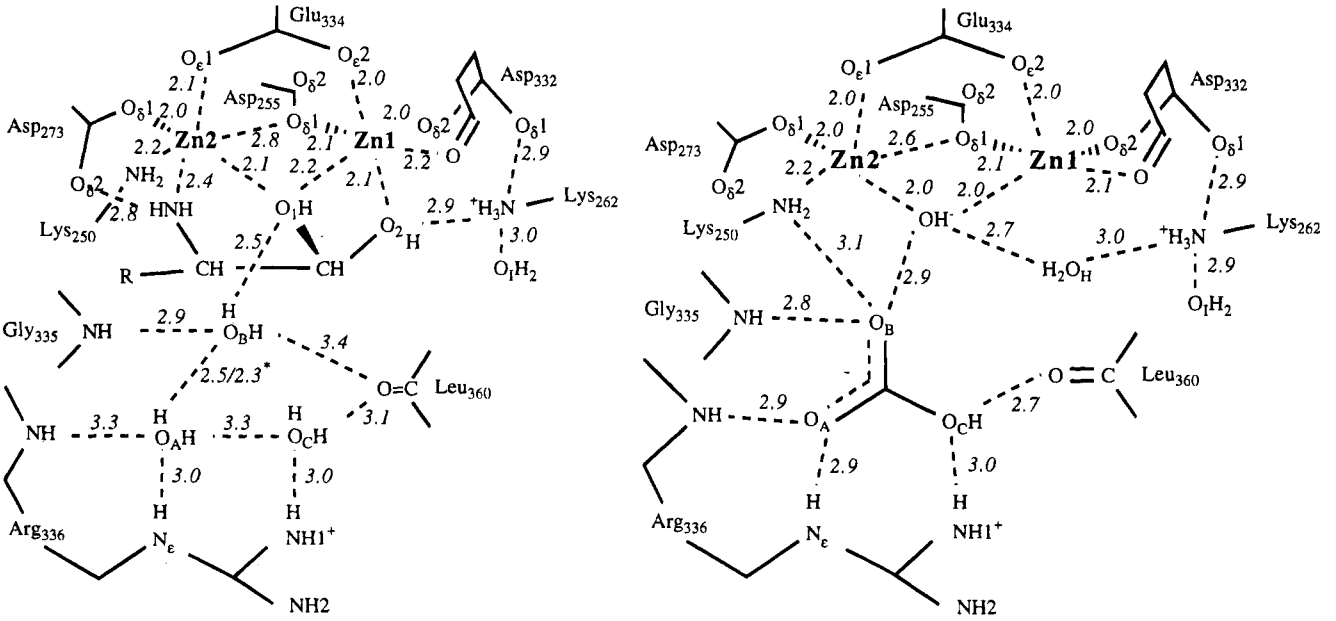

FIGURE 4: Interactions in the active site of blLAP complexed with leucinal (left) and in unliganded blLAP (right). Selected interatomic distances of hydrogen bonds and coordinating bonds are given in angstroms. Additional distances are listed in Table 2. (Asterisk) The distance of 2.3 Å between waters A and B in the blLAP–leucinal complex was obtained from a refinement without force-field restraints for the nonbonded interactions for these two water molecules.

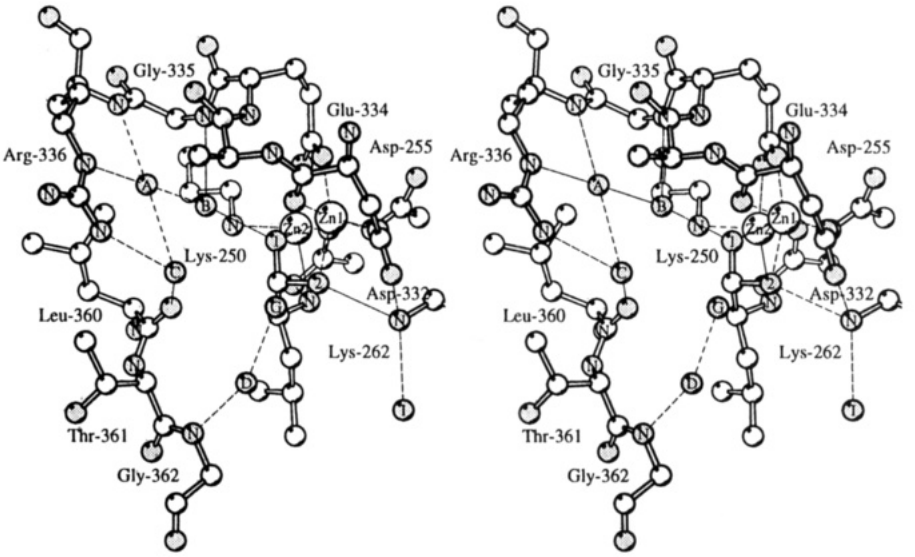

FIGURE 5: Active site structure of blLAP complexed with leucinal. Besides the zinc ions, leucinal, and the amino acids, the positions of six water molecules (A−D, G, I) are shown. Metal coordination and hydrogen bonds are represented as thin, dashed lines. Oxygen and nitrogen atoms are shown in gray. The view is approximately from the central solvent cavity of the blLAP hexamer into the active site of one subunit.

Table 2: Selected Interatomic Distances (Å)[a]

atom blLAP−leucinal/native	atom	blLAP−leucinal	blLAP−native
O1, leucinal/O_J, water	N_ζ, Lys-250	3.2	3.2
N, leucinal	N_ζ, Lys-250	3.7	
O_A, water/O_A, carbonate	C_δ1, Leu-360	3.4	3.7
O_A, water/O_A, carbonate	N, Glu-334	4.0	3.4
O_A, water/O_A, carbonate	N, Gly-335	3.6	3.1
O_A, water/O_A, carbonate	C_α, Ala-333	3.5	3.2
O_A, water/O_A, carbonate	C, Ala-333	3.5	3.0
O_B, water/O_B, carbonate	N, Glu-334	3.7	3.6
O_B, water/O_B, carbonate	C_δ1, Leu-360	3.6	3.6
O_B, water/O_B, carbonate	O, Leu-360	3.4	3.7
O_B, water	O_C, water	3.7	
O_B, water/O_B, carbonate	N_ζ, Lys-250	3.1	3.1
O_C, water/O_C, carbonate	O_G, water	3.6	>4
O_C, water/O_C, carbonate	C_γ2, Thr-361	3.7	>4
O_D, water	O_H, water		3.7
O_K, water	O_δ2, Asp-273		3.3
O_H, water	O_K, water		2.8
Zn1	O_H, water		3.7

[a] In addition to the distances given in Figure 4.

in the blLAP and blLAP−leucinal structures, respectively. This metal ion probably serves a structural role and has been described previously (Sträter & Lipscomb, 1995).

$F_o - F_c$ electron density maps of the unliganded enzyme revealed the presence of one water ligand coordinated to the di-zinc core (Figure 6). This water molecule or hydroxide ion bridges both metal ions and is very close to the position of the bridging OH group of the bound inhibitors bestatin, amastatin, LeuP, and leucinal in the corresponding structures. No positive electron density feature was apparent near Zn1 at the position of O2 in the leucinal and LeuP inhibitor structures. The metal-coordinated water molecule is hydrogen bonded to water H, which also displays a hydrogen bond to Lys-262. The $F_o - F_c$ electron density map also revealed a strong triangular density island between Arg-336 and the di-zinc cluster. When three water molecules were placed in these positions and refined without force field restraints between each other and with the protein, distances of 2.1, 1.8, and 1.8 Å for A to B, A to C, and B to C, respectively, were derived.[2] There was also positive density present in the middle of the three density peaks. The strong and well-defined density of Arg-336, the strong density of the triangular density feature, and the absence of any continuous density between Arg-336 and the density island clearly show that this density is not caused by alternate conformations of Arg-336. It seems most probable that a planar anion of XO_3 geometry has bound here. Since there were no such anions added to the crystallization buffer, this density (peaks A−C) is most likely caused by a bicarbonate ion, which was present in the crystallization buffer from dissolved CO_2 or from carbonate in the sodium hydroxide which was employed during the isolation procedure. The carbonate ion fits well into the density, and all atoms were refined to *B*-factors lower than 13 Å^2. The carbonate ion displays several hydrogen bonds to active site residues including a hydrogen bond to the hydroxide ion bridging the zinc ions (Figures 4 and 5).

In order to establish whether the presence of bicarbonate shows any influence on blLAP catalysis, the enzyme activity was determined at various concentrations of $NaHCO_3$ at pH 7.8. Sodium bicarbonate displays noncompetitive or mixed inhibition of LAP-catalyzed hydrolysis of L-leucine-*p*-nitroanilide, and the inhibition constant was determined as 120 mM. No activitation was found at lower bicarbonate concentrations.

DISCUSSION

Inhibitor and Transition State Binding Modes. The binding mode of leucinal is very similar to that of LeuP (Figure 8). The two *gem*-diol oxygen atoms coordinate in the same way to the di-zinc center as do two of the three phosphoryl oxygen atoms of LeuP. Due to the longer C−P and P−O bond lengths in LeuP, the two zinc ions are pushed farther apart (3.4 Å) compared to the distance in the blLAP−leucinal complex (3.1 Å). It is mainly Zn1 which moves upon inhibitor binding. The carboxylate side chain of Asp-

[2] The peaks A−C refer to maxima in the electron density map of Figure 6 at the positions of O_A, O_B, and O_C of the modeled carbonate ion.

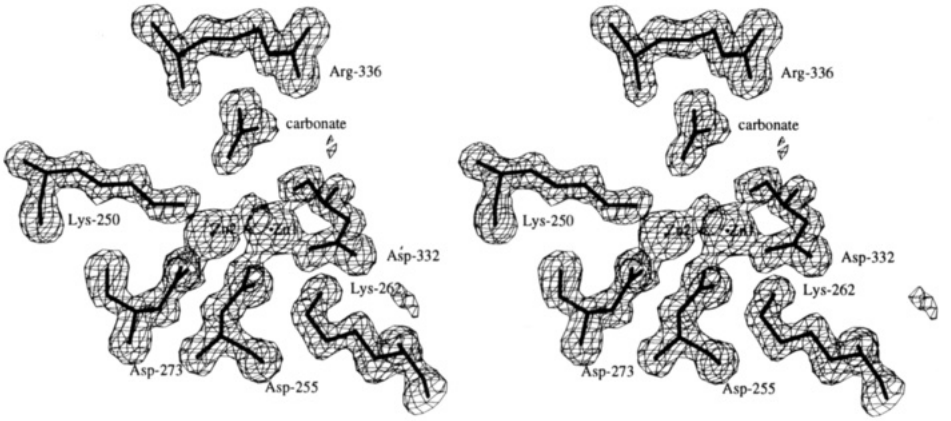

FIGURE 6: $F_o - F_c$ electron density map of selected active site residues of unliganded blLAP. The residues shown in this figure have been omitted from the model in the calculation of the density map. For clarity, the side chain of Glu-334 is not shown here. The contour level of the map is $3\sigma_{rms}$.

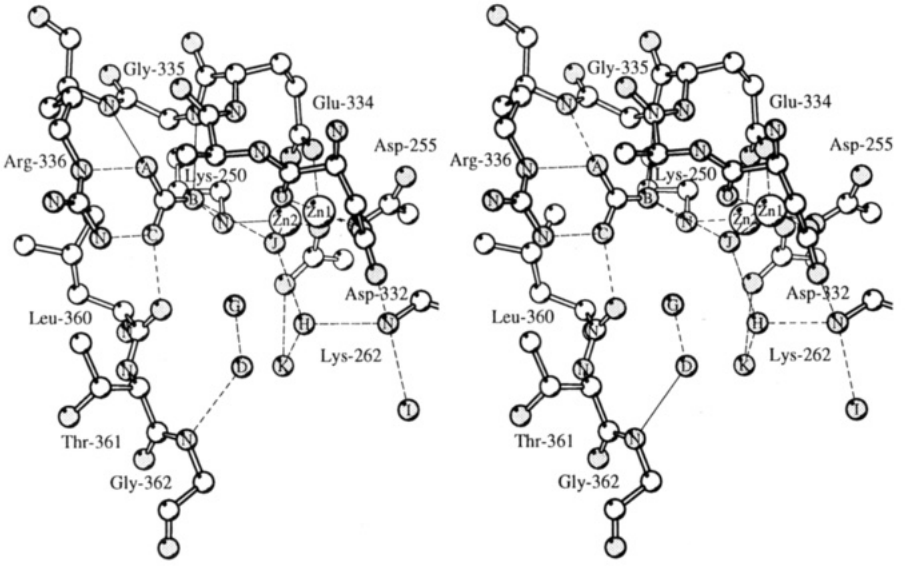

FIGURE 7: Structure of the active site of unliganded blLAP. Shown are the two zinc ions, the active site amino acid residues, the presumed carbonate or bicarbonate ion, and six water molecules (D, G−K). Water molecule J bridges both zinc ions. The oxygen atoms of the carbonate ion have been labeled A−C, corresponding to the water positions A−C in the blLAP−leucinal and the blLAP−LeuP structures. However, the refined water positions in the blLAP−leucinal and the blLAP−LeuP structures are significantly further apart than the oxygen atoms of the carbonate ion (Figure 4, Table 2).

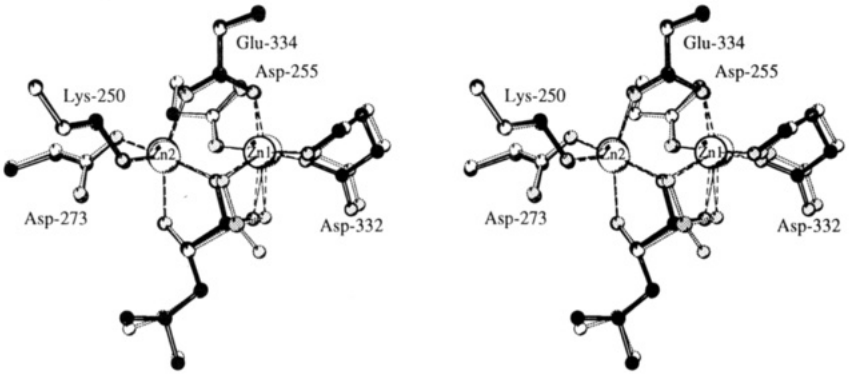

FIGURE 8: Superposition of the di-zinc centers and the bound inhibitors in the blLAP−leucinal and the blLAP−LeuP structures. The leucinal complex is shown in solid lines, and the carbon atoms are drawn in black. The structure of the LeuP complex is represented as dashed lines, and the carbon atoms are white. The coordinating bonds are drawn as thin, dashed lines.

332 follows this movement. These findings thus confirm the conclusions drawn from the blLAP−LeuP inhibitor structure, namely, that probably three atoms of the tetrahedral *gem*-diolate transition state or intermediate are coordinated to the di-metal center: these atoms include the terminal amino group of the substrate coordinated to Zn2 and two of the three oxygen/nitrogen atoms around the former carbonyl carbon atom. The similar binding mode of leucinal and LeuP also demonstrates that the weaker binding constant of the phosphorus-containing amino acid analogue is due to the different electronic and steric properties of these two compounds and is not the result of a different binding mode.

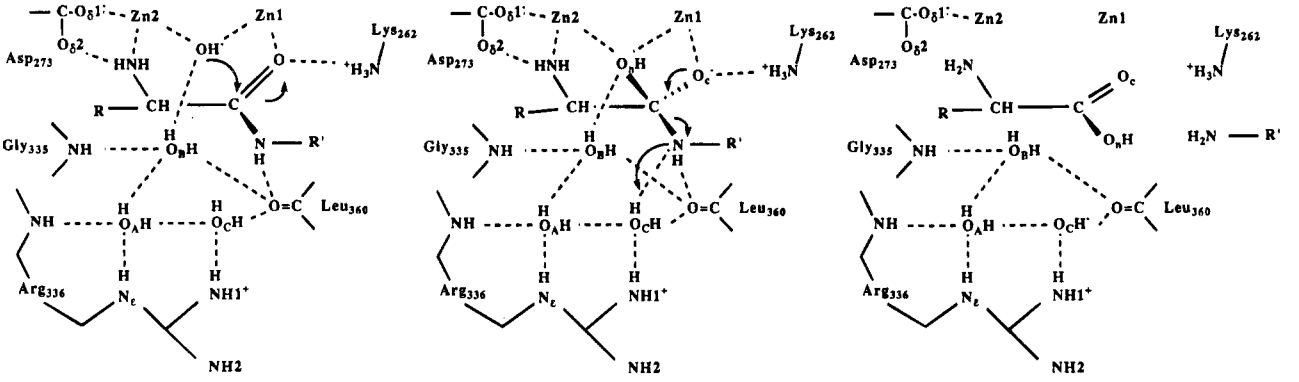

FIGURE 9: Proposed pathway for LAP catalysis. Hydrogen bonds and coordinating bonds are shown as dashed lines. O_n is the oxygen atom of the former nucleophile, and O_c is the oxygen from the former peptide carbonyl O. The mechanism is discussed in the text.

The inhibition constant of LeuP to porcine kidney LAP is 0.23 μM.

Mechanism of Catalysis. Although the binding mode of leucinal to blLAP is similar to that of LeuP, it also contributes new information to the discussion of blLAP catalysis: if one assumes that both *gem*-diolate oxygen atoms of leucinal bind in the same way as the *gem*-diolate oxygen atoms of the intermediate, then either mechanism I or mechanism II (Figure 2) could be the correct pathway. On the basis of the binding mode of LeuP, which bears three oxygen atoms around the phosphorus atom, it was also speculated that the former peptide nitrogen atom of the substrate may interact with Zn1 to facilitate the release of the leaving group (mechanism III in Figure 2). However, it was already noted that this is a less probable alternative since the binding mode of bestatin and amastatin indicates that the peptide nitrogen of the substrate most likely binds near the atom position of O3 in the blLAP–LeuP structure (Sträter & Lipscomb, 1995). The binding mode of leucinal confirms the view that the former peptide nitrogen atom in the intermediate does not coordinate to Zn1, and it supports mechanisms I and II.

Mechanisms I and II differ in the substrate binding mode and in the location of the OH^- nucleophile. Since the high-resolution structure of unliganded blLAP showed that no water molecule is coordinated to Zn1 at the position of the water nucleophile as proposed in mechanisms II and III, it seems reasonable to assume that the water or hydroxide ion bridging both metal ions is the nucleophile in LAP catalysis. The structures of the unliganded enzyme and the structures with transition state analogue inhibitors support the following mechanism (Figure 9). The substrate binds to the di-zinc core of LAP with the terminal amino group coordinated to Zn2 and the carbonyl group coordinated to Zn1. The binding causes an increase of the coordination number of both zinc ions—no metal-bound water ligands have to be displaced. However, the substrate does displace water molecules D, G, and H (Figure 7). The displacement of water molecule H, which was hydrogen bonded to the zinc-bound nucleophile, destabilizes the hydroxide ion and enhances its nucleophilicity. The carbonyl group is polarized by coordination to Zn1 and by the hydrogen bond from Lys-262. After attack of the hydroxide ion, a *gem*-diolate intermediate is formed. The energy of this intermediate or transition state complex is lowered by the coordination of both *gem*-diolate oxygens to the di-zinc center. In addition, the presumably negatively charged oxygen O_c of the former carbonyl group is stabilized by a hydrogen bond from the protonated side chain of Lys-262. Water molecule B contributes a hydrogen bond to the *gem*-diolate oxygen O_n. The breakdown of the intermediate upon elimination of the P1′ amino group is facilitated by a hydrogen bond from water molecule C, which protonates the leaving group. This water molecule is polarized by Arg-336.

In the crystal structure of *Aeromonas proteolytica* aminopeptidase (AAP), the two active site zinc ions are also bridged by a water ligand (Chevrier et al., 1994), which is the only water molecule (or hydroxide anion) which could be located in the di-zinc coordination sphere in the 1.8 Å electron density map. The bridging water is hydrogen bonded to three additional active site water molecules. There have been no structures published yet of an enzyme–inhibitor complex for AAP, and therefore the proposed catalytic mechanisms for these two aminopeptidase cannot be compared. The active site structure of AAP differs significantly from that of blLAP; a striking feature of the AAP dinuclear metal center is the structural similarity of the coordination spheres around the two zinc ions.

The triangular density between Arg-336 and the dinuclear zinc site in the unliganded enzyme is most probably caused by a bicarbonate or a carbonate ion. The three density maxima are too close together to be interpreted as three water molecules. Both the strong electron density and the low *B*-factors indicate that these atomic positions are fully occupied. The presence of alternate water positions seems highly unlikely since an average occupancy of only one-third would be expected for each of the positions. Moreover, this binding site also seems well suited for the binding of a HCO_3^- or CO_3^{2-} ion (Figures 4, 6). No activation of the enzyme by $NaHCO_3$ was detected in this work, and activation has also not been reported in previous studies of LAP catalysis. Thus, it seems unlikely that a carbonate ion plays an active role in the enzymatic mechanism. The carbonate ion is most probably displaced when the substrate binds to the active site. The enzyme is inhibited by relatively high concentrations of $NaHCO_3$, but it is unclear whether this inhibition is caused by binding to the site next to Arg-336.

Water molecules A and B are very close together in the blLAP–leucinal structure, especially when the water molecules are refined only on the basis of the experimental X-ray data without nonbonded interactions. A similar short distance of 2.3 Å (or 2.1 Å in the independent second subunit of the asymmetric unit) between these active site water molecules was found in the inhibitor complex of blLAP with LeuP determined at 1.65 Å resolution (Sträter & Lipscomb,

1995).[3] The strength of the peaks in the electron density in both structures and the relatively low *B*-factors do not indicate that these water positions are alternately occupied. The three independent observations of this distance and the high resolution of the X-ray data in both structures suggest that these small distances are significant and not artifacts of the error limit in the coordinates.[4]

Short, presumably strong hydrogen bonds are discussed for a number of enzymic reactions in the stabilization of the transition state (Cleland, 1992; Gerlt & Gassman, 1993a,b; Cleland & Kreevoy, 1994). The existence and character of these hydrogen bonds in enzymic catalysis are currently a controversial issue (Warshel et al., 1995; Scheiner & Kar, 1995). A very short hydrogen bond of 2.3 Å has been found in the bihydroxide ($[HOHOH]^-$) ion in a crystal structure where this ion is surrounded by four water molecules (Abu-Dari et al., 1979a,b). It is conceivable that this ion is stabilized in the pocket next to Arg-336 by the influence of the positively charged arginine side chain and the zinc ions as well as by the hydrogen bond donors surrounding this pocket. The hydrogen atom of O1 of leucinal as shown in Figure 4 has no hydrogen bonding partner. If water B is deprotonated, the O_1H hydroxyl group may contribute a hydrogen bond toward this water molecule. The distance between O1 of leucinal and water B has also been refined to a relatively small value of 2.5 Å; however, the existence of an unusually short hydrogen bond is less clear for this interaction because the distance is closer to that of a normal hydrogen bond. Short hydrogen bonds between an active site carboxylate group and a zinc-bound water molecule or a zinc-coordinated oxygen atom of an inhibitor have also been observed in cytidine deaminase (Xiang et al., 1995), carboxypeptidase A (Kim & Lipscomb, 1990, 1991), and thermolysin (Matthews, 1988). The *gem*-diolate intermediate differs from leucinal in the overall negative charge and in the presence of the amino leaving group. At present, we do not know whether this short hydrogen bond distance between the two water peaks is relevant to catalysis by LAP. If one assumes that a bihydroxide ($H_3O_2^-$) anion is indeed stable at the binding site next to Arg-336 in the unliganded enzyme or in the presence of bound substrate, perhaps it helps to create the OH^- nucleophile which attacks the scissile peptide bond. However, this type of activation of a water nucleophile is to our knowledge unprecedented in any proposed mechanism for hydrolytic enzymes, and the current experimental evidence is too vague to support this alternative at this stage.

An alternative explanation for the short distance between waters A and B is that this short distance is a result of static disorder of the water molecules in the direction of the short distance, i.e., that in a small percentage of the enzyme active sites in the crystal only one water molecule (or possibly also two oxygens of an otherwise disordered carbonate ion) would be bound between the positions of waters A and B. Refining two water molecules at A and B would then result in a distance that is biased toward values which are too small because the putative disorder was not modeled appropiately.

[3] In the blLAP–LeuP structure, water molecules A and B were refined without interactions between one another.

[4] If an error of 0.2 Å is assumed for the atom coordinates based on the error estimation from the Luzzati plot, then a standard deviation of about 0.3 Å can be expected for the distance between the two water molecules.

The two new crystal structures presented herein allow a choice between the three alternative pathways previously proposed for LAP catalysis. In conjunction with published structural and biochemical data, both structures support mechanism 1 (Figures 2 and 9). The blLAP–leucinal cocrystal structure in conjuction with the high-resolution structure of the native enzyme also resolves the question as to whether Arg-336 participates in blLAP catalysis by being present in alternate conformations. Both structures strongly implicate that Arg-336 is present only in one conformation and interacts with the intermediate via water molecules, as previously indicated by the blLAP–LeuP structure. However, these structures also raise some new questions; first, concerning the identity and relevance of the density island near Arg-336 in the unliganded enzyme, which is most probably a bound bicarbonate ion. Another open question is the cause and mechanistic relevance of the short hydrogen bond between active site water molecules A and B, and possibly between water B and atom O1 of leucinal.

ACKNOWLEDGMENT

We are grateful to Mr. Jason Altom and Prof. Elias J. Corey for their constant support and advice during the synthesis of leucinal. Also, Prof. Richard Wolfenden is acknowledged for providing information on leucinal synthesis and stability.

REFERENCES

Abu-Dari, K., Freyberg, D. P., & Raymond, K. N. (1979a) *Inorg. Chem. 18*, 2427–2433.

Abu-Dari, K., Raymond, K. N., & Freyberg, D. P. (1979b) *J. Am. Chem. Soc. 101*, 3688–3689.

Allen, M. P., Yamada, A. H., & Carpenter, F. H. (1983) *Biochemistry 22*, 3778–3783.

Andersson, L., Isley, T. C., & Wolfenden, R. (1982) *Biochemistry 21*, 4177–4180.

Andersson, L., MacNeela, J., & Wolfenden, R. (1985) *Biochemistry 24*, 330–333.

Brünger, A. T. (1992a) *X-PLOR Manual*, Version 3.1, Yale University, New Haven, CT.

Brünger, A. T. (1992b) *Nature 355*, 472–475.

Burley, S. K., David, P. R., Taylor, A., & Lipscomb, W. N. (1990) *Proc. Natl. Acad. Sci. U.S.A. 87*, 6878–6882.

Burley, S. K., David, P. R., & Lipscomb, W. N. (1991) *Proc. Natl. Acad. Sci. U.S.A. 88*, 6916–6920.

Burley, S. K., David, P. R., Sweet, R. M., Taylor, A., & Lipscomb, W. N. (1992) *J. Mol. Biol. 224*, 113–140.

Carpenter, F. H., & Harrington, K. Y. (1972) *J. Biol. Chem. 247*, 5580–5586.

Carpenter, F. H., & Vahl, J. M. (1973) *J. Biol. Chem. 248*, 294–304.

Chevrier, B., Schalk, C., D'Orchymont, H., Rondeau, J., Moras, D., & Tarnus, C. (1994) *Structure 2*, 283–291.

Cleland, W. W. (1992) *Biochemistry 31*, 317–319.

Cleland, W. W., & Kreevoy, M. M. (1994) *Science 264*, 1887–1890.

Delange, R. J., & Smith, E. L. (1971) in *The Enzymes* (Boyer, P. D., Ed.) 3rd ed., Vol. III, pp 81–119. Academic Press, New York.

Gerlt, J. A., & Gassman, P. G. (1993a) *J. Am. Chem. Soc. 115*, 11552–11568.

Gerlt, J. A., & Gassman, P. G. (1993b) *Biochemistry 32*, 11943–11952.

Hanson, H., & Frohne, M. (1976) *Methods Enzymol. 45*, 504–521.

Ito, A., Takahashi, R., & Baba, Y. (1975) *Chem. Pharm. Bull. 23*, 3081–3087.

Jones, T. A., & Kjeldgaard, M. (1994) in *From First Map to Final Model. Proceedings of the CCP4 Study Weekend* (Bailey, S.,

Hubbard, R., & Waller, D., Eds.) pp 1−13, Daresbury Laboratory, Warrington, U.K.
Jurnak, F., Rich, A., van Loon-Klaassen, L., Bloemendal, H., Taylor, A., & Carpenter, F. (1977) *J. Mol. Biol. 112*, 149−153.
Kabsch, W. (1988) *J. Appl. Crystallogr. 21*, 67−71.
Kim, H., & Lipscomb, W. N. (1990) *Biochemistry 29*, 5546−5555.
Kim, H., & Lipscomb, W. N. (1991) *Biochemistry 30*, 8171−8180.
Kim, H., & Lipscomb, W. N. (1993a) *Biochemistry 32*, 8465−8478.
Kim, H., & Lipscomb, W. N. (1993b) *Proc. Natl. Acad. Sci. U.S.A. 90*, 5006−5010.
Kim, H., & Lipscomb, W. N. (1994) *Adv. Enzymol. 68*, 153−213.
Kraulis, P. (1991) *J. Appl. Crystallogr. 24*, 946−950.
Luzzati, P. V. (1952) *Acta Crystallogr. 5*, 802−810.
Matthews, B. W. (1988) *Acc. Chem. Res. 21*, 333−340.
Melbye, S. W., & Carpenter, F. H. (1971) *J. Biol. Chem. 246*, 2459−2463.
Molecular Simulations Inc. (1994) *QUANTA*, V. 4.0, Burlington, MA.
Moriya, T., Yoneda, N., Miyoshi, M., & Matsumoto, K. (1982) *J. Org. Chem. 47*, 94−98.
Roderick, S. L., & Matthews, B. W. (1993) *Biochemistry 32*, 3907−3912.
Scheiner, S., & Kar, T. (1995) *J. Am. Chem. Soc. 117*, 6970−6975.
Smith, E. L., & Hill, R. L. (1960) in *The Enzymes* (Boyer, P. D., Lardy, H., & Myrback, K., Eds.) 2nd ed., Vol. 4, Part A, pp 37−63, Academic Press, New York.
Taylor, A. (1993a) *Trends Biochem. Sci. 18*, 167−172.
Taylor, A. (1993b) *FASEB J. 7*, 290−298.
Taylor, A., Daims, M. A., Lee, J., & Surgenor, T. (1982) *Curr. Eye Res. 2*, 47−56.
Thompson, G. A., & Carpenter, F. H. (1976a) *J. Biol. Chem. 251*, 53−60.
Thompson, G. A., & Carpenter, F. H. (1976b) *J. Biol. Chem. 251*, 1618−1624.
Umezawa, H. (1980) *Recent Results Cancer Res. 75*, 115−125.
Warshel, A., Papazyan, A., Kollman, P. A., Cleland, W. W., Kreevoy, M. M., & Frey, P. A. (1995) *Science 269*, 102−106.
Xiang, S., Short, S. A., Wolfenden, R., & Carter, C. W. (1995) *Biochemistry 34*, 4516−4523.

BI951746Q